The EMBO Journal Vol. 21 No. 5 pp. 1101–1111, 2002

Hyperacetylation of chromatin at the *ADH2* promoter allows Adr1 to bind in repressed conditions

Loredana Verdone[1], Jiansheng Wu[2], Kristen van Riper[3], Nataly Kacherovsky[3], Maria Vogelauer[2], Elton T.Young[3], Michael Grunstein[2], Ernesto Di Mauro[1,4] and Micaela Caserta[4,5]

[1]Fondazione Istituto Pasteur-Fondazione Cenci Bolognetti and [4]Centro di Studio per gli Acidi Nucleici, CNR, c/o Dipartimento di Genetica e Biologia Molecolare, Università La Sapienza, I-00185 Rome, Italy, [2]Department of Biological Chemistry, UCLA School of Medicine and Molecular Biology Institute, University of California, Los Angeles, CA 90095 and [3]Department of Biochemistry, Box 357350, University of Washington, Seattle, WA 98195-7350, USA

[5]Corresponding author
e-mail: micaela.caserta@uniroma1.it

We report that *in vivo* increased acetylation of the repressed *Saccharomyces cerevisiae ADH2* promoter chromatin, as obtained by disrupting the genes for the two deacetylases *HDA1* and *RPD3*, destabilizes the structure of the TATA box-containing nucleosome. This acetylation-dependent chromatin remodeling is not sufficient to allow the binding of the TATA box-binding protein, but facilitates the recruitment of the transcriptional activator Adr1 and induces faster kinetics of mRNA accumulation when the cells are shifted to derepressing conditions.

Keywords: *ADH2*/chromatin remodeling/histone acetylation/*Saccharomyces cerevisiae*/transcriptional regulation

Introduction

Regulation of gene expression by chromatin structure is well established in eukaryotes. The involvement of ATP-dependent chromatin remodeling complexes and of acetylation/deacetylation in gene activation and/or repression has been clearly shown (Kingston and Narlikar, 1999; Kornberg and Lorch, 1999; Vignali *et al*., 2000; Wu and Grunstein, 2000). Most of the initial evidence came from genetic studies correlating loss of activation and/or repression with specific mutations in chromatin remodeling complexes and/or acetyltransferases and deacetylases (Hirschhorn *et al*., 1992; Peterson and Herskowitz, 1992; Braunstein *et al*., 1993; Rundlett *et al*., 1996; Kadosh and Struhl, 1998; Kuo *et al*., 1998; Struhl, 1998). These genetic analyses were followed by biochemical studies showing the *in vitro* effects of these modifying complexes (Hamiche *et al*., 1999; Längst *et al*., 1999; Lorch *et al*., 1999; Travers, 1999; Whitehouse *et al*., 1999; Aalfs and Kingston, 2000) on nucleosome structure. Additional studies have added to this matter the analysis of the acetylation levels of specific genomic regions in order to relate the effect of the modification of specific lysine residues to specific patterns of expression. For example, it was shown that transcriptional repression by *UME6* involves *RPD3*-dependent deacetylation of histone H4 (Rundlett *et al*., 1998; Suka *et al*., 2001) and that cell cycle-regulated histone acetylation is required for the expression of the yeast *HO* gene (Krebs *et al*., 1999), while *TUP1* utilizes histone H3/H2B-specific *HDA1* deacetylase to repress transcription (Wu *et al*., 2001). Moreover, it was proposed that targeted histone acetylation by Gcn5 facilitates transcription in a causal fashion (Kuo *et al*., 2000). In general, promoter histone acetylation is differentially affected by specific activators and repressors (Deckert and Struhl, 2001). A detailed analysis of almost 54 kb of DNA in a search of developmentally regulated patterns of histone acetylation was presented recently (Litt *et al*., 2001). In addition to targeted histone modification, a background of global acetylation and deacetylation was reported (Kuo *et al*., 2000; Vogelauer *et al*., 2000), indicating that the state of acetylation of a genome is in constant flux.

What is still missing in this field is an understanding at the molecular level of the direct effect of *in vivo* changes in histone acetylation on gene expression. Do changes in histone proteins lead directly to physical changes in nucleosome structure and promoter utilization? An attempt in this direction was recently made in the *PHO8* promoter system (Reinke *et al*., 2001). Interestingly, a transient hyperacetylation peak over the *PHO8* promoter, limited to precisely those nucleosomes that are remodeled upon activation, is induced by SAGA; nevertheless, the evidence presented points against a direct effect of acetylation on chromatin accessibility *in vivo*.

In order to determine whether histone acetylation affects promoter accessibility, we chose as a model system the *Saccharomyces cerevisiae ADH2* gene, coding for the enzyme alcohol dehydrogenase II, in its natural chromosomal location. This gene is tightly regulated by glucose and becomes active when the glucose concentration of the medium is lowered or in the presence of non-fermentable carbon sources. An upstream regulatory element (UAS1; Beier and Young, 1982), which binds the transcription factor Adr1 (Denis and Young, 1983), is required for its derepression. We have previously shown that when yeast cells are grown in repressing conditions (3% glucose), two nucleosomes (–1 and +1) occupy the basic promoter elements: the TATA box and the RNA initiation sites (RIS), respectively (Verdone *et al*., 1996). UAS1 is located in a nucleosome-free region, but one of the two Adr1-binding sites is immediately adjacent to the upstream borders of the TATA box-containing –1 nucleosome. A relevant role for the two nucleosomes in the maintenance of transcriptional repression is shown by the fact that by blocking the production of histone H4 *in vivo*, and therefore the correct assembly of the nucleosome particles,

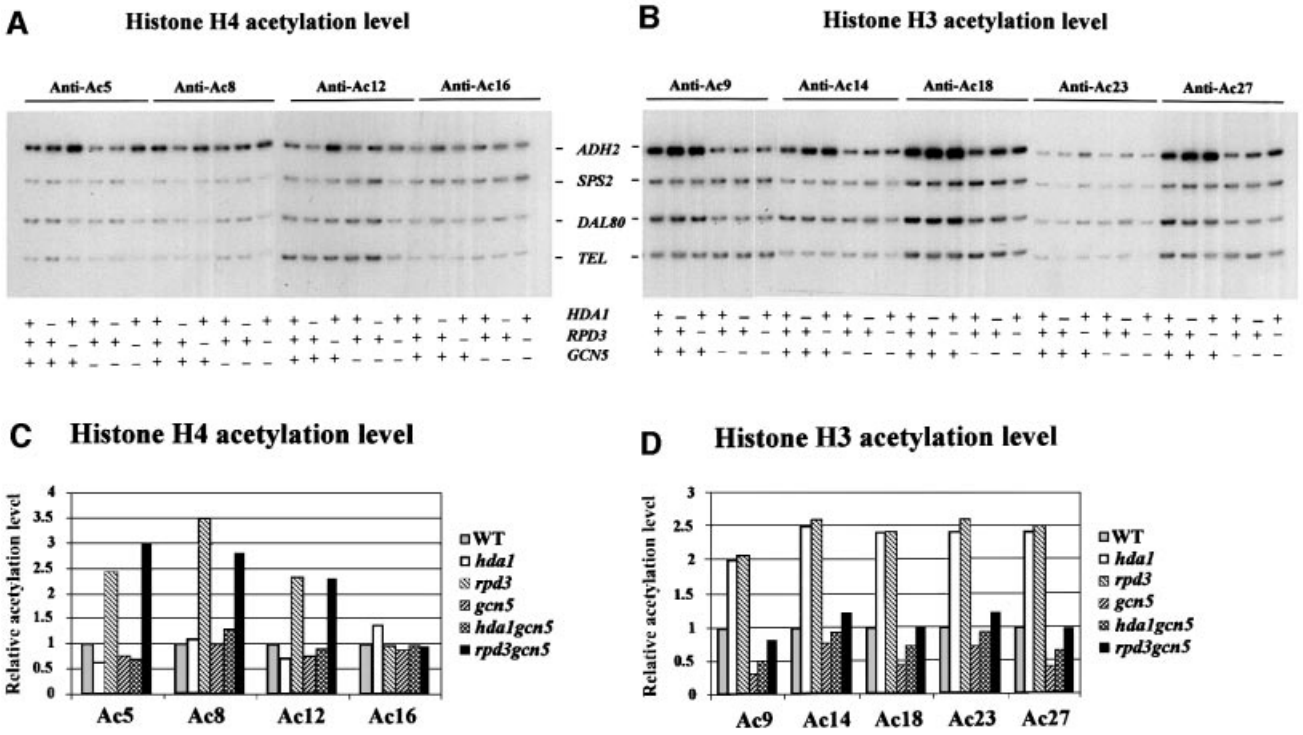

Fig. 1. Effects of histone acetyltransferase *GCN5* and histone deacetylases *HDA1* and *RPD3* on acetylation of histones at the *ADH2* promoter. ChIP demonstrating the effects of histone acetyltransferase and histone deacetylase disruptions on the acetylation of (**A**) histone H4 sites K5, K8, K12 and K16, and (**B**) histone H3 sites K9, K14, K18, K23 and K27. The *ADH2* fragment spans the region from –223 to +114, relative to the ATG. Amplification of a 138 bp fragment 0.5 kb from the telomere (Tel) of chromosome VI-R was used as a reference to ensure equal loading of samples. Yeast strains used for ChIP were wild type (WT) (YDS2), *hda1* (WJY111), *rpd3* (WJY140), *gcn5* (WJY139), *hda1*/*gcn5* (WJY142) and *rpd3*/*gcn5* (WJY143) (Vogelauer *et al*., 2000). *SPS2* and *DAL80* were found to be relatively unaffected by these mutations and were used as negative controls. (**C** and **D**) Quantification of the increase in H4, H3 acetylation in mutant cells relative to wild-type cells. [α-^{32}P]dATP was added to the PCR mixture, and the PhosphorImager was used to quantitate the intensity of *ADH2* PCR bands in these mutants relative to WT after normalizing to the *TEL* bands.

ADH2 becomes active even in the presence of glucose (Wyrick *et al*., 1999). When yeast cells are grown in low glucose (0.05%), the two promoter nucleosomes, together with other adjacent particles, undergo *ADR1*-dependent chromatin remodeling and transcriptional activation (Verdone *et al*., 1996, 1997; Di Mauro *et al*., 2000).

In order to understand the role of histone acetylation in *ADH2* gene expression, it is necessary to demonstrate that acetylation alters chromatin structure and that the acetylation-dependent nucleosome structural modifications influence the ability of the promoter to be activated.

By genetically altering the steady-state pattern of histone acetylation at the repressed *ADH2* promoter, we show that when the histone deacetylases *HDA1* and *RPD3* are mutated, the structure of the TATA box-containing nucleosome is destabilized, the promoter becomes accessible to Adr1, and, when the cells are shifted to derepressing conditions, the kinetics of mRNA accumulation is faster. We also show that by disrupting the genes for the two acetyltransferases *GCN5* and *ESA1*, the *ADH2* promoter structure and function are affected. In particular, in the *GCN5* mutant, the chromatin remodeling occurring in derepressing conditions is less pronounced and the kinetics of mRNA accumulation is slower, whereas in the presence of an *ESA1* temperature-sensitive mutation, the amount of mRNA is lower even in permissive conditions. Therefore, histone deacetylation/acetylation is directly involved in modulating the accessibility of chromatin at the *ADH2* gene.

Results

The histone acetylation level of the ADH2 promoter changes when the deacetylases HDA1 and RPD3 and the acetyltransferases ESA1 and GCN5 are not functional

We started our analysis by searching for a direct effect on the *ADH2* histone acetylation level of disruptions in the genes coding for the two major *S.cerevisiae* histone acetyltransferases, *GCN5* (a component of both the SAGA and the ADA complexes; Grant *et al*., 1997) and *ESA1* (a member of the NuA4 complex; Smith *et al*., 1998; Allard *et al*., 1999; Clarke *et al*., 1999), and in the genes for the two deacetylases *HDA1* and *RPD3*. The study was performed by chromatin immunoprecipitation (ChIP) analysis of a region encompassing the basic transcription elements, the TATA box and the RNA initiation sites, occupied by nucleosomes –1 and +1, respectively (see the diagram in Figure 3 and Verdone *et al*., 1997). Figures 1 and 2A and B show the results obtained by PCR amplification of a 337 bp *ADH2* fragment relative to a 138 bp fragment, 0.5 kb from the telomere (Tel) of chromosome VI-R, used as an internal control for the quantity of DNA. Nine different antibodies were used (five specific for the histone H3 acetylated lysines AcK9, AcK14, AcK18, AcK23 and AcK27, and four specific for the histone H4 acetylated lysines AcK5, AcK8, AcK12 and AcK16) to immunoprecipitate formaldehyde-cross-

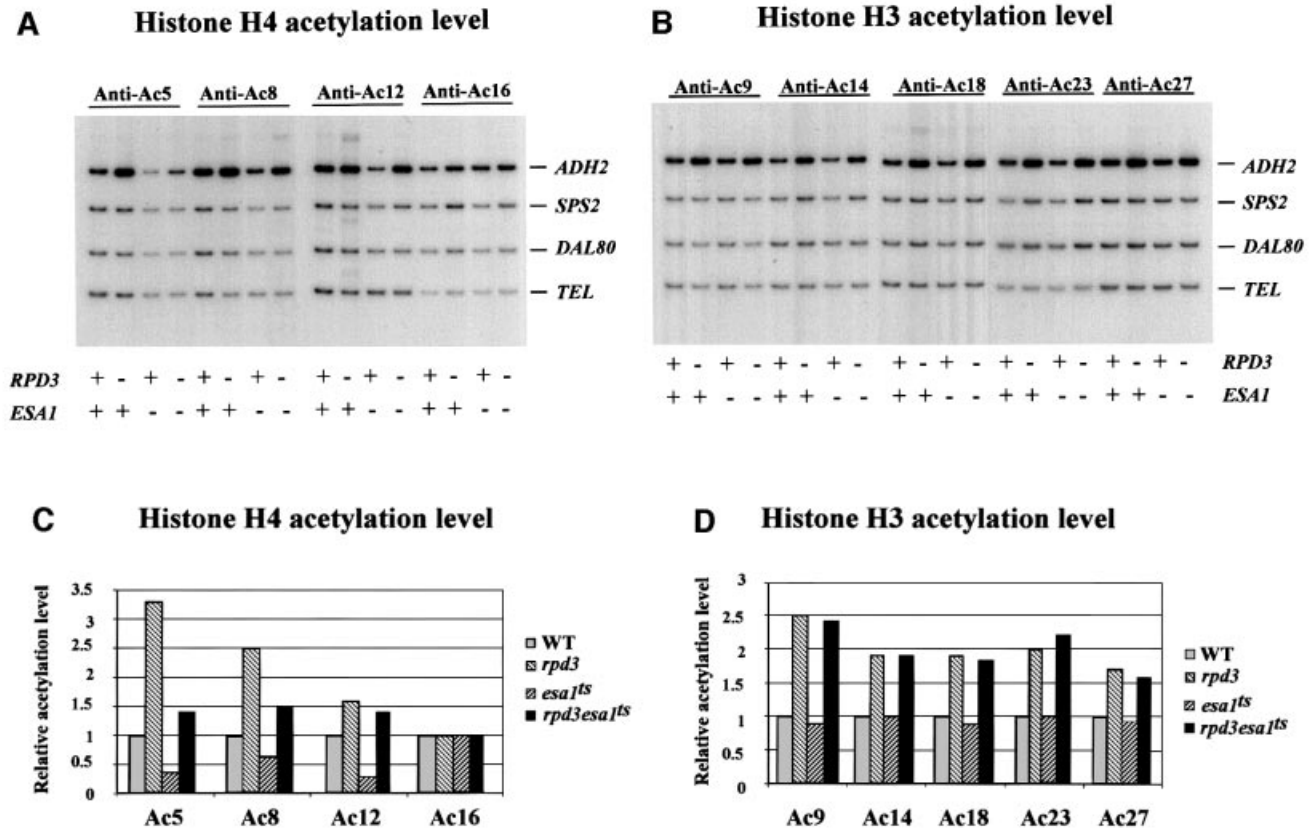

Fig. 2. Effects of histone acetyltransferase *ESA1* on acetylation of histones at the *ADH2* promoter. ChIP demonstrating the effects of histone acetyltranferase *esa1*^{ts} mutant on the acetylation of (**A**) histone H4 sites K5, K8, K12 and K16, and (**B**) histone H3 sites K9, K14, K18, K23 and K27. The *ADH2* fragment spans the region from –223 to +114, relative to the ATG. Amplification of a 138 bp fragment 0.5 kb from the telomere (Tel) of chromosome VI-R was used as a reference to ensure equal loading of samples. Yeast strains used for ChIP were WT (LPY3431), *rpd3* (NSY164), *esa1*^{ts} (LPY3430), *rpd3*/*esa1*^{ts} (NSY165). *SPS2* and *DAL80* were found to be relatively unaffected by these mutations and were used as negative controls. (**C** and **D**) Quantification of the increase in H4, H3 acetylation in mutant cells relative to wild-type cells. [α-^{32}P]dATP was added to the PCR mixture, and the PhosphorImager was used to quantitate the intensity of *ADH2* PCR bands in these mutants relative to WT after normalizing to the *TEL* bands.

linked chromatin of different cell extracts prepared from cultures grown in 3% glucose, i.e. in repressing conditions for *ADH2* expression. The quantitative evaluation of these data is reported in Figures 1 and 2C and D; the histone acetylation level for each mutant strain is shown relative to the wild-type level, equivalent to 1. In the case of histone H4, it is clear that *RPD3* deacetylates three out of the four lysines (K5, K8 and K12; Figure 1C) and that the same residues are acetylated by *ESA1* (Figure 2C). In fact, the hyperacetylation observed in the *rpd3* mutant is abolished in the double mutant *rpd3*/*esa1*^{ts} (Figure 2C), but not in the double mutant *rpd3*/*gcn5* (Figure 1C). In the case of histone H3, both *RPD3* and *HDA1* deacetylate the five lysines (K9, K14, K18, K23 and K27; Figure 1D) that are acetylated by *GCN5* (Figure 1D). In fact, the hyperacetylation observed in the *hda1* and *rpd3* single mutants is abolished in the double mutants *hda1*/*gcn5* and *rpd3*/*gcn5* (Figure 1D). Moreover, *GCN5* does not acetylate the histone H4 lysines because the hyperacetylation shown in the *rpd3* mutant is not abolished in the double mutant *rpd3*/*gcn5* (Figure 1C), and *ESA1* does not acetylate the histone H3 lysines because the hyperacetylation shown in a second *rpd3* mutant is not abolished in the double mutant *rpd3*/*esa1*^{ts} (Figure 2D).

From these data we can conclude that the histone acetylation level of the *ADH2* promoter is directly affected by disrupting the two main acetyltransferases *GCN5*, which is H3 specific, and *ESA1*, which is H4 specific, and the deacetylases *HDA1*, which is H3 specific, and *RPD3*, which is specific for both H3 and H4. How do all these covalent modifications affect the structure of the nucleosomes present at the promoter and therefore the ability of the *ADH2* gene to be activated?

Histone deacetylation/acetylation is directly involved in modulating the structure of the TATA box-containing nucleosome

In order to assess the influence of the changes in the acetylation level on the structure of the nucleosomes present in the repressed *ADH2* promoter in its natural chromosomal location, we analyzed by indirect end labeling the micrococcal nuclease (MN) digestion pattern in a set of isogenic strains carrying single, double or triple disruptions in the genes coding for the main histone deacetylases and acetyltransferases. The results are shown in Figure 3. Increasing amounts of MN were introduced by nystatin permeabilization of the spheroplasts obtained from cells grown in repressing (R = 3% glucose)

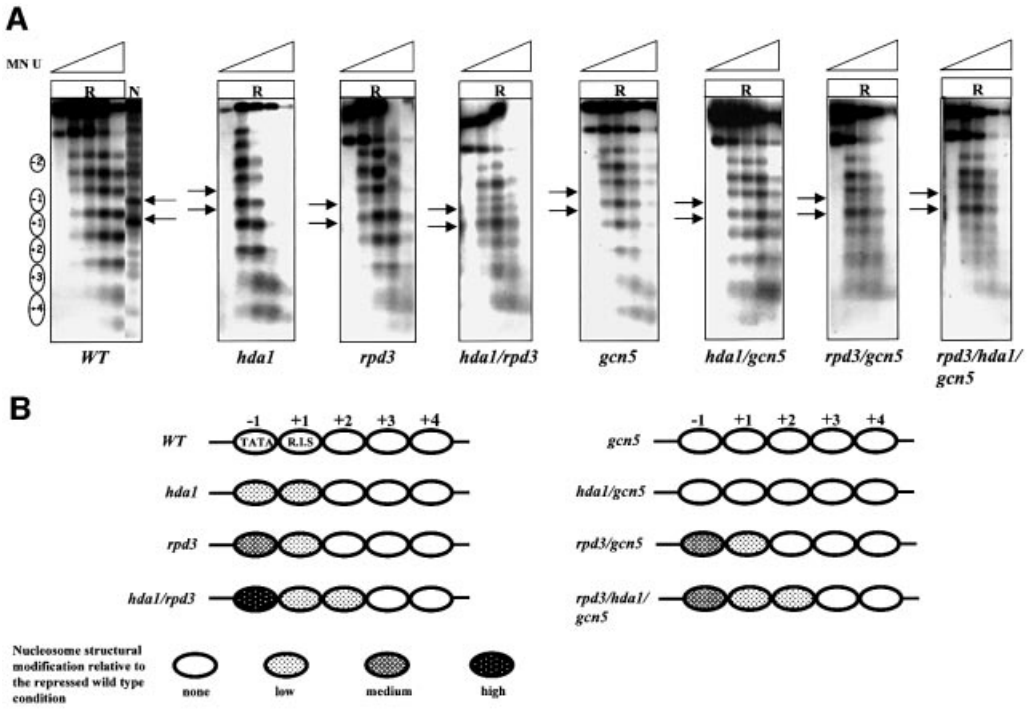

Fig. 3. Effects of histone acetylation on *ADH2* chromatin structure. (**A**) MN analysis of the *ADH2* promoter region in repressing conditions (R, 3% glucose). Nystatin-permeabilized spheroplasts were reacted with increasing amounts of MN (U = units/0.25 ml: 0, 0.57, 1.7, 5 and 15), deproteinized, digested with *Bam*HI and *Hin*dIII (map positions are –1202 and +760, respectively), and analyzed by indirect end-labeling. Nucleosomes (i.e. protected areas) are represented as ovals. Lane N (naked control) contains deproteinized DNA from plasmid pFA treated *in vitro* with MN and the same restriction enzymes as the *in vivo* samples. (**B**) Summary of nucleosome structural modifications. The chromatin changes, relative to the wild-type YDS2 strain, are summarized; the different shadings indicate the intensity of the changes (none, low, medium and high).

conditions. The pattern of *in vivo* MN cleavage sites is compared with that of an *in vitro* treated sample (lane N = naked chromosomal DNA) in order to reveal the protection from DNA cleavage due to the presence of nucleosomes. In the case of the wild-type strain, an array of nucleosomes covering the entire area of the promoter and the surrounding regions (with the exception of a nucleosome-free region located between particles –2 and –1; see Verdone *et al*., 1996) is clearly visible.

When looking at the MN profiles of both the *rpd3* and *hda1* mutants, we noted a slight modification in the ability of the promoter nucleosomes –1 and +1 to protect the underlying DNA sequence (Figure 3). The loosened structure of these nucleosomes is more clearly seen in the case of the *hda1*/*rpd3* double mutant, suggesting that the hyperacetylation observed on both histones H3 and H4 in the absence of *RPD3* and/or *HDA1* (caused by the histone acetyltransferase activity of *GCN5* and *ESA1*, respectively; see Figures 1 and 2) is responsible for the partial loss of protection of the *ADH2* basic promoter elements.

When the nucleosome structure is analyzed in the *gcn5* mutant, the MN profile is very similar to that of the wild type, suggesting that the H3 hypoacetylation characteristic of this mutant (Figure 1C) helps to keep the promoter chromatin in a relatively inaccessible configuration.

When combined with *hda1*, the *gcn5* disruption behaves as a suppressor; in fact, the *hda1*/*gcn5* strain is characterized by a chromatin structure very similar to that of the wild type and of the single *gcn5* mutant strain, with an array of tightly associated nucleosomes over the promoter (Figure 3). The implication is that the hypoacetylation of histone H3 in the *hda1*/*gcn5* double mutant is responsible for the suppression of the partial opening of the nucleosome –1 structure, characteristic of the *hda1* mutant (Figure 3).

In the double mutant *rpd3*/*gcn5*, the –1 nucleosome is characterized by a loosened structure typical of the *rpd3* mutant, suggesting that in repressing conditions the *gcn5* disruption does not suppress the *rpd3* phenotype.

In the case of the triple mutant *rpd3*/*hda1*/*gcn5*, the delicate balance among the various acetyltransferases and deacetylases is such that in repressing conditions the chromatin structure is loosened (Figure 3, last panel); in fact, the *gcn5* disruption only partially suppresses the phenotype due to the double *hda1*/*rpd3* disruption.

A diagram showing the results of the chromatin analysis in repressing conditions for the entire set of mutants is presented in Figure 3B.

Histone deacetylation/acetylation affects Adr1 but not TATA box-binding protein (TBP) access to the ADH2 promoter in repressing conditions

Adr1 is the major transcription factor binding in the nucleosome-free region upstream of the –1 nucleosome when cells are derepressed. Whether Adr1 is present during repressed growth in a chromatin-bound but transcriptionally inactive form, or is not bound to chromatin, has not been resolved. If the latter were the case, destabilization of nucleosome –1 might allow Adr1

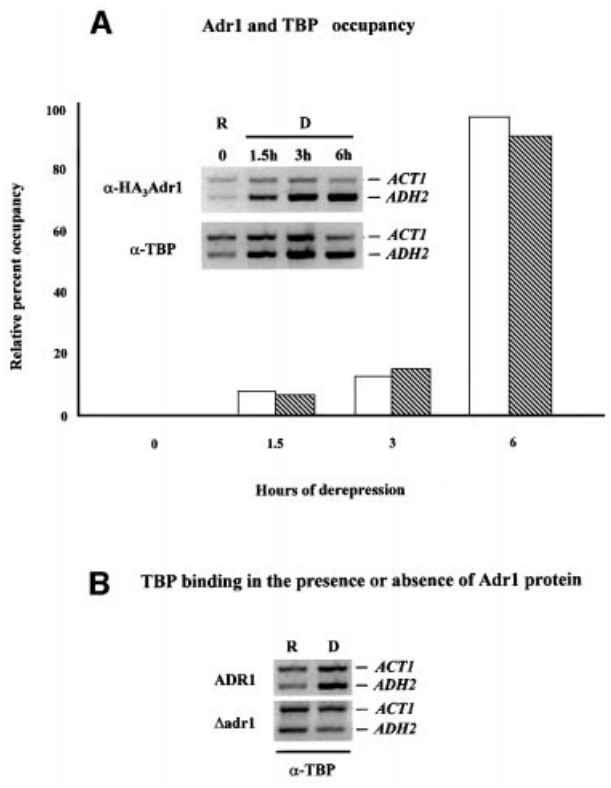

Fig. 4. Adr1 and TBP occupancy of the *ADH2* promoter. (**A**) ChIP assays for Adr1-HA and TBP were performed with anti-HA and anti-yTBP, respectively, as described in Materials and methods. The primer pairs for the PCR analysis, followed by gel electrophoresis (inset), are located at –432 and –139 from the *ADH2* ATG. The primer pairs for the *ACT1* control were located at +418 and +797 in the *ACT1* ORF. Real-time PCR analysis was carried out with an Applied Biosystems Model 700 and software as described by the manufacturer. The primer pairs for the real-time PCR analysis are located at –283 and –187 from the *ADH2* ATG. The primer pairs for the ACT1 control were located at +448 and +531 in the *ACT1* ORF. The real-time PCR data are shown in the graph and are plotted as a percent of the *ADH2* product generated using ChIP DNA isolated from repressed cells, after correcting for the amount of *ACT1* DNA in each sample (white and hatched bars refer to Adr1 and TBP occupancy, respectively). R, repressed conditions (3% glucose); D, derepressed conditions (0.05% glucose). (**B**) ChIP assays for TBP occupancy in wild-type and *adr1* strains. PCR and electrophoretic analysis were carried out as described in Materials and methods and in (A).

to bind UAS1 even in the presence of glucose, and this could lead to more rapid derepression of *ADH2* expression.

To test this possibility we performed ChIP using a strain containing an HA epitope-tagged version of Adr1 that behaved identically to the wild-type allele. The data shown in Figure 4A indicate that Adr1 is not bound to the *ADH2* promoter in glucose-repressed cells containing a full complement of deacetylases. Adr1 can be detected at the *ADH2* promoter ~90 min after the cells are shifted to medium lacking glucose, and the amount of Adr1 at the promoter continues to increase until at least 6 h, as measured by real-time PCR of the immunoprecipitated DNA. When the arrival of TBP at the *ADH2* promoter is determined, it appears to coincide with the appearance of Adr1 (Figure 4A), suggesting that its recruitment is *ADR1* dependent. Consistent with this interpretation, TBP cannot be detected at the *ADH2* promoter in a strain lacking Adr1 (Figure 4B). These results show: (i) that Adr1 is not bound to the ADH2 promoter during glucose repression and recruits TBP upon derepression; and (ii) that Adr1 must be present at the promoter for TBP to bind.

We reasoned that the destabilization of the TATA box-containing nucleosome –1, observed in the deacetylase mutants (Figure 3), could influence the ability of members of the transcription machinery or of the activator itself to bind *in vivo* their target sites in repressed growth conditions, when neither Adr1 nor TBP was normally bound to the *ADH2* promoter. We therefore analyzed by ChIP with anti-Adr1 or anti-yTBP antibodies the occupancy of the *ADH2* UAS1 and TATA box region by Adr1 and TBP, respectively, in four different strains: wild type, *rpd3*, *gcn5* and *rpd3*/*hda1*. The results are shown in Figure 5. All the extracts were prepared from cells grown in 3% glucose (repressing conditions) and the immunoprecipitated material was amplified by PCR with different pairs of oligonucleotides. As a negative control for unspecifically immunoprecipitated material, we included a fragment (*ADH2* ORF) containing a small portion of the *ADH2* coding region, located between 800 and 900 bp from the TATA box. The positive control for TBP binding is a fragment (*ACT1* TATA) containing the TATA box of the *ACT1* gene, which is constitutively expressed in high-glucose conditions (Figure 5A). The results show that there is no change in TBP binding efficiency at the *ADH2* promoter when comparing the various mutants with the wild type (Figure 5B). In particular, there is no increase in TBP occupancy for the *ADH2* TATA box fragment relative to the *ADH2* ORF fragment when comparing the deacetylase mutants with the wild-type strain, suggesting that the hyperacetylation-dependent increased accessibility to MN of the TATA box-containing nucleosome is not affecting the accessibility of the promoter to the transcription machinery. On the other hand, when testing the anti-Adr1 antibody with the same extracts, we observed an increase in the occupancy of the ADH2 promoter by Adr1 in the *hda1*/*rpd3* double mutant (Figure 5C). The quantitative evaluation of these data is presented in Figure 5D.

We conclude that the destabilization of the TATA box-containing –1 nucleosome even in high-glucose conditions (i.e. in the absence of transcription) induces the binding of Adr1 to the promoter, but not the recruitment of TBP, suggesting that the access of the transcriptional activator to its target sites represents an essential but not sufficient regulatory step for *ADH2* derepression, since in repressed conditions TBP is still not recruited despite the presence of Adr1.

These data show that the exact pattern of covalent modifications of the promoter nucleosome, and therefore its precise structural organization, has an important role in the control of Adr1 activator chromosomal localization.

Increased histone acetylation determines faster kinetics of ADH2 promoter transcriptional activation, while decreased histone acetylation causes slower kinetics of derepression

In order to assess the influence of changes in the acetylation level on the expression of our model gene, we analyzed by northern blotting the kinetics of *ADH2* mRNA accumulation in the same set of isogenic mutant strains for which the chromatin analysis was performed.

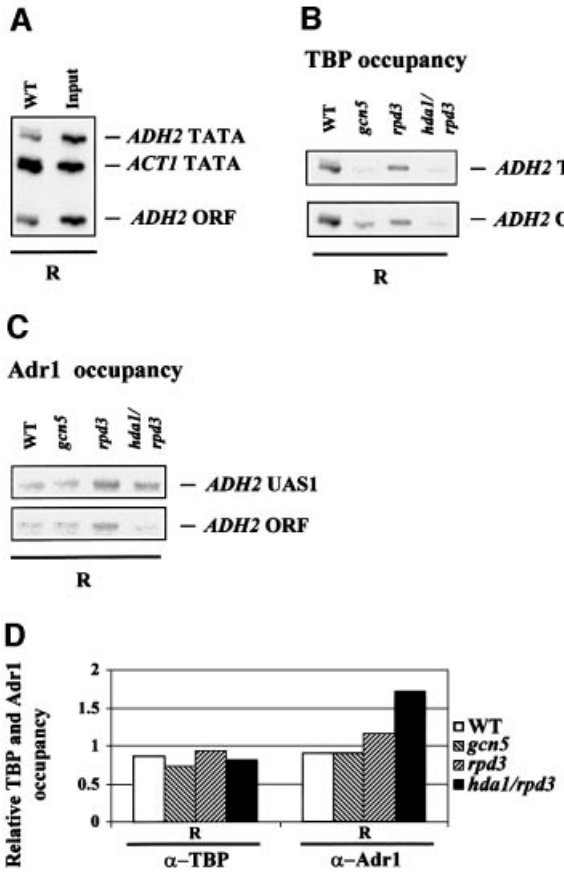

Fig. 5. Acetylation-dependent Adr1 binding of the repressed *ADH2* promoter. (**A**) Positive control for TBP binding. DNA immunoprecipitated with anti-yTBP (α-TBP) from wild-type extract under repressing conditions (R) and input DNA derived from the same extract were amplified with three different pairs of oligonucleotides at the same time: *ADH2* TATA fragment (234 bp) spans the region from –223 to +11; *ACT1* TATA fragment (182 bp) contains the *ACT1* TATA box; *ADH2* ORF fragment (108 bp) contains a small portion of the *ADH2* coding region from +658 to +778 (negative control). Amplifications were performed using the following amounts of DNA: WT = 1/50; Input = 1/2500. (**B**) ChIP with anti-yTBP antibody illustrating the occupancy of the *ADH2* TATA box region by TBP in the WT, *gcn5*, *rpd3* and *hda1*/*rpd3* strains, in repressing conditions (R). The TBP-immunoprecipitated material was amplified by PCR with two different pairs of oligonucleotides at the same time. (**C**) ChIP with anti-Adr1 antibody (α-Adr1) demonstrating the occupancy of the *ADH2* promoter in the WT, *gcn5*, *rpd3* and *hda1*/*rpd3* strains in repressing conditions (R). The Adr1-immunoprecipitated material was amplified by PCR with two different pairs of oligonucleotides at the same time. The *ADH2* UAS1 fragment (217 bp) spans the region from –379 to –162. (**D**) Densitometric evaluation of the results shown in (B) and (C). The histograms were obtained by dividing the values of the *ADH2* TATA and of the *ADH2* UAS1 fragments by the value of the *ADH2* ORF fragment, used as a negative control.

Figure 6 shows the results of this analysis; for each mutant, the *ADH2* mRNA was tested in the initial repressed conditions (*R* = 3% glucose) and at different times (from 30 min up to 6 h) after decreasing the amount of glucose in the medium to 0.05%. When comparing the kinetics of both the *hda1* and *rpd3* mutants with those of the wild type, a faster derepression is observed: the *ADH2* mRNA is already present at 30 min after the shift to derepressing conditions, suggesting a role in the transcriptional activation process for the increased histone acetylation caused by the absence of *HDA1* or *RPD3*. The effect of the increased acetylation caused by the absence of the two deacetylases is additive; in fact, when comparing the kinetics of the double mutant *hda1*/*rpd3* with that of each single mutant, the *ADH2* mRNA signal at 30 min after the shift is stronger and equivalent to the sum of the signals at 30 min of each single mutant (see also the densitometric evaluation in Figure 6C). This additive effect, due to the hyperacetylation of both histones H3 and H4, correlates with the stronger chromatin modification seen in the case of the *hda1*/*rpd3* double mutant (see Figure 3). We have also analyzed the mRNA accumulation at a shorter time (10 min) after the shift to derepressing conditions: the *ADH2* signal is already visible in the *rpd3* and *hda1* strains, but not in the wild type, and it is even stronger in the *hda1*/*rpd3* strain (data not shown).

On the other hand, when the kinetics of the *gcn5* mutant is analyzed, there is no signal of *ADH2* mRNA accumulation up to 3 h after the shift, suggesting a role for the *GCN5*-dependent histone acetyltransferase activity in the initial step of transcriptional activation at this promoter. When combined with the *hda1* mutation, the *gcn5* disruption behaves as a suppressor; in fact, the kinetics of mRNA accumulation in the *hda1*/*gcn5* strain is very similar to those of the single *gcn5* strain, with no signal up to 3 h after the shift. The implication is that the faster kinetics of *ADH2* derepression observed in the *hda1* mutant is due to *GCN5*-mediated hyperacetylation. Instead, when combined with the *rpd3* mutation, the *gcn5* disruption appears to behave as a suppressor only at 1 and 2 h after the shift, whereas at 30 min the faster kinetics due to the absence of *RPD3* is the predominant effect. The implication is that the faster kinetics of derepression, observed in the absence of *RPD3* only, is due to an increased acetylation level partly mediated by *GCN5* and partly by a different histone acetyltransferase, presumably *ESA1*.

In the triple mutant *rpd3*/*hda1*/*gcn5*, the delicate balance among the various acetyltransferases and deacetylases is such that at 30 min and 1 h after the shift, a low *ADH2* mRNA level is visible. However, at 2–3 h after the shift, the mRNA signal is reduced with respect to the double *rpd3*/*gcn5* mutant, and at the same time a reduced extent of chromatin remodeling is observed (data not shown).

We have also studied the effect of an *esa1* temperature-sensitive mutant on *ADH2* transcription; the results are shown in Figure 6D and E. The effect of the *esa1* mutation should be visible only at the restrictive temperature (37°C); nevertheless, it appears that the mutant *esa1* protein does not behave normally even at the permissive temperature (28°C). In fact, the *ADH2* mRNA level is always lower in the mutant when compared with the wild type both at 28 and 37°C, suggesting a role for the *ESA1*-mediated promoter acetylation in the transcriptional process.

From this set of data, we conclude that the change in acetylation level, observed at the *ADH2* promoter in each mutant relative to the wild type, correlates not only with a defined pattern of nucleosome structural alterations, but also with a change in the kinetics of mRNA accumulation.

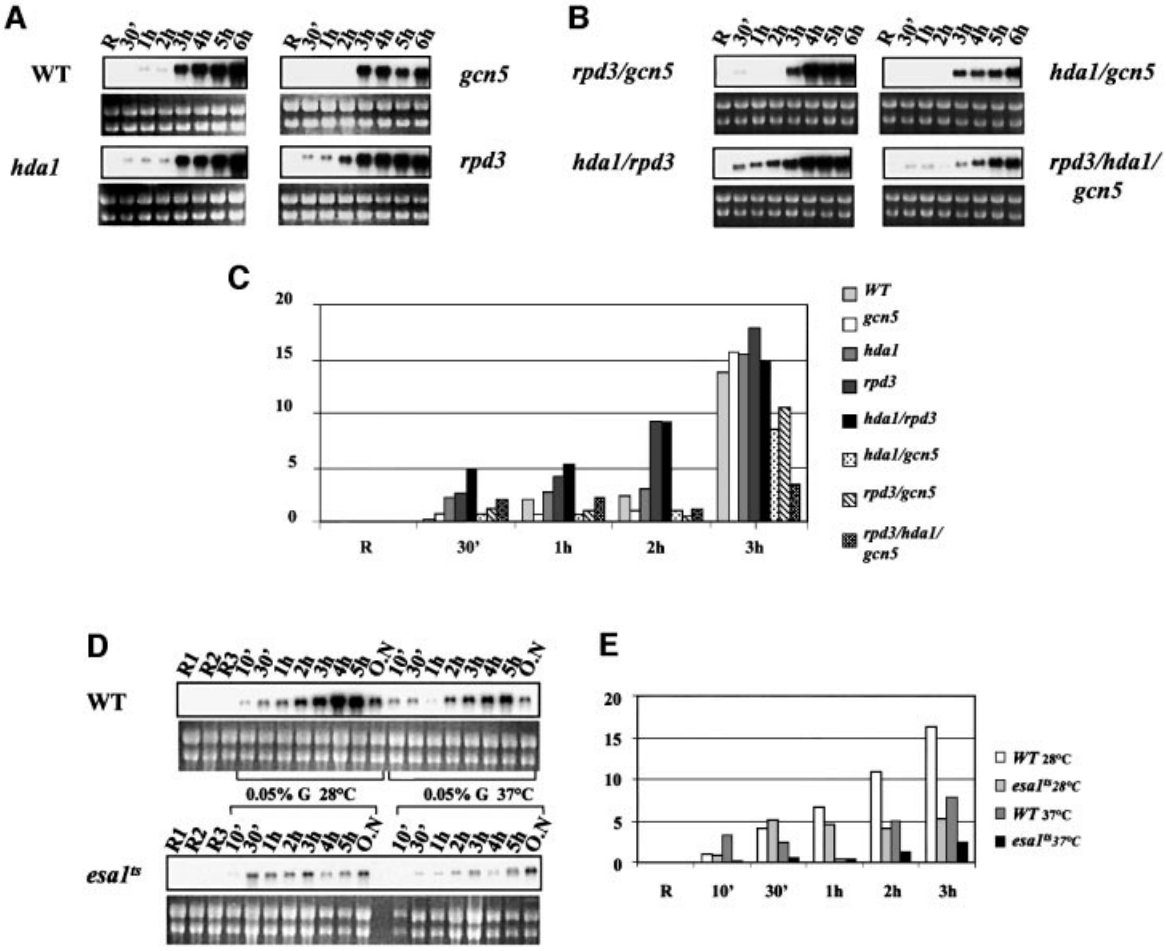

Fig. 6. Effects of histone acetylation on the kinetics of *ADH2* mRNA accumulation. (**A** and **B**) Northern analysis for the wild-type YDS2 strain and the mutants indicated. Cells were grown overnight in repressing conditions (3% glucose, lanes R), washed, resuspended in fresh medium containing 0.05% glucose and analyzed at the times indicated. (**C**) Histogram representing the densitometric evaluation of the results shown in (A) and (B), from R (repressing condition) up to 3 h. (**D**) Northern analysis for the wild-type LPY3430 and its isogenic *esa1*^{ts}. Cells were grown overnight at 28°C in repressing conditions (R1 lanes). The culture was split into two: one flask was kept at 28°C, the other was shifted to 37°C for 8 h in order to inactivate Esa1 (Clarke *et al*., 1999). The same amount of cells from each culture was analyzed (R2 = 28°C; R3 = 37°C). After Esa1 inactivation, the cells were washed and resuspended in fresh medium containing 0.05% glucose and analyzed at the times indicated (from 10 min to overnight). (**E**) Histogram representing the densitometric evaluation of the results shown in (D), from the initial repressing conditions (R = R1, R2, R3) up to 3 h.

The acetyltransferase Gcn5 is required for efficient chromatin remodeling during derepression

The analysis of the MN profiles of the wild-type and *gcn5* mutant strains in repressing conditions did not reveal any difference (Figure 3), even though the histone H3 acetylation level was lower in the mutant when compared with the wild type (Figure 1D). However, the different acetylation pattern is responsible for the slower kinetics of mRNA accumulation observed in the *gcn5* strain (Figure 6). We therefore also analyzed the *ADH2* promoter chromatin structure in derepressing conditions in the wild-type and *gcn5* strains. The results are shown in Figure 7. At 3 h after the shift to derepressing conditions, some differences become evident: (i) the intensity of the MN induced bands appearing inside all particles present on both the promoter and the coding region, very high in the case of the wild type, is reduced in the *gcn5* mutant; and (ii) the intensity of the MN induced bands at the borders of all nucleosomes is very similar when going from repressing to derepressing conditions in the *gcn5* mutant, whereas it is strongly reduced in the wild type after the metabolic shift.

The results are consistent with a reduced ability of the *ADH2* nucleosomes to undergo chromatin remodeling in the absence of the *GCN5*-dependent histone acetyltransferase activity.

Discussion

Histone acetylation state regulates ADH2 promoter chromatin structure and transcription

We have analyzed the *in vivo* chromatin structure and the kinetics of transcriptional activation of the *S.cerevisiae ADH2* promoter as a function of genetically modified histone acetylation levels.

In an exponentially growing wild-type strain in the presence of glucose (repressing conditions for the *ADH2* gene), an equilibrium exists among the various histone acetyltransferases and deacetylases. When this equilibrium is altered by abolishing the function of either or both

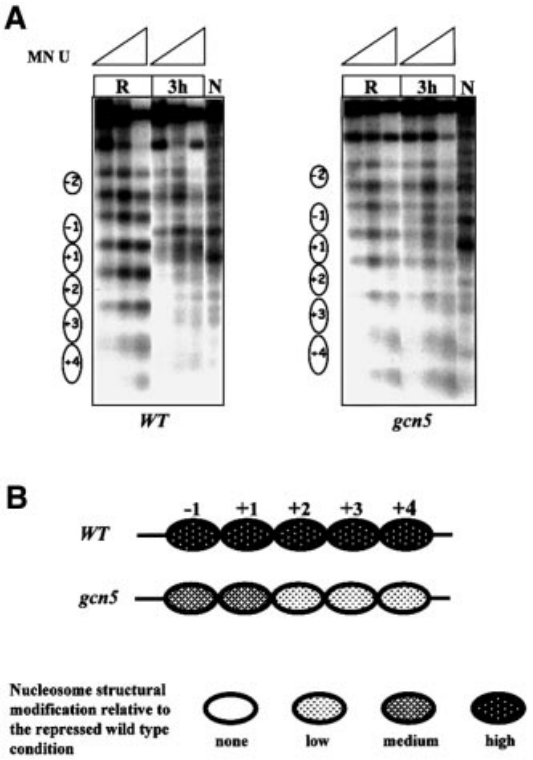

Fig. 7. Role of the acetyltransferase Gcn5 in *ADH2* promoter chromatin remodeling. (**A**) MN analysis of the *ADH2* promoter region in repressing conditions (R, 3% glucose) and at 3 h after the shift to derepressing conditions (3 h, 0.05% glucose). Nystatin-permeabilized spheroplasts, of both wild-type and *gcn5* strains, were reacted with increasing amounts of MN (U = units/0.25 ml: 0.57, 1.7 and 5), deproteinized, digested with *Bam*HI and *Hin*dIII (map positions are –1202 and +760, respectively), and analyzed by indirect end-labeling. Nucleosomes (i.e. protected areas) are represented as ovals. Lanes N (naked control) contain deproteinized DNA from plasmid pFA treated *in vitro* with MN and the same restriction enzymes as the *in vivo* samples. (**B**) Summary of nucleosome structural modifications. The chromatin changes in the *gcn5* strain, relative to the wild-type YDS2 strain, are summarized; the different shadings indicate the intensity of the changes (none, low, medium and high).

RPD3 and *HDA1*, an imbalance is created, leading to hyperacetylation of specific lysine residues, thus causing specific modifications of the structure of both nucleosomes –1 and +1 (see Figure 3). The partial loss of protection observed does not induce mRNA synthesis in repressing conditions, but is responsible for inducing a defined timing for the synthesis of the *ADH2* mRNA when the cells are shifted to derepressing medium (0.05% glucose). In particular, faster kinetics of mRNA accumulation is obtained when either or both *RPD3* and *HDA1* genes are disrupted (see Figure 6).

On the other hand, when the equilibrium is altered by abolishing the activity of the acetyltransferase Gcn5, the ability of histone H3 to be correctly acetylated is compromised. In repressing conditions, the structures of nucleosomes –1 and +1 appear very similar to the wild-type situation, whereas in derepressing conditions the reduced acetylation causes a decreased extent of chromatin remodeling, leading to slower kinetics of activation.

When combined with *hda1*, the *gcn5* disruption behaves as a suppressor; in fact, the *hda1*/*gcn5* strain is characterized by a chromatin structure very similar to that of the wild type and of the single *gcn5* mutant strain, with an array of tightly associated nucleosomes over the promoter (Figure 3). The implication is that the hypoacetylation of the histone H3 in the *hda1*/*gcn5* double mutant is responsible for the suppression of the partial opening of the nucleosome –1 structure, characteristic of the *hda1* mutant (Figure 3). This suppressor effect is also reflected at the functional level: the kinetics of mRNA accumulation, faster in the single *hda1* mutant, become slower in the *hda1*/*gcn5* strain (see Figure 6).

The effects of a *gcn5* disruption combined with an *rpd3* disruption are more complex. Since *RPD3* deacetylates both histones H3 and H4 (Figure 1), the most likely interpretation of the data regarding the double mutant *rpd3*/*gcn5* is that the dominant *rpd3* mutant effect seen in repressing conditions on the –1 nucleosome structure (Figure 3) and on mRNA synthesis very soon (30 min) after the shift to derepressing conditions (see Figure 6) is due to histone H4 hyperacetylation, whereas the dominant *gcn5* mutant effect on both transcription (see Figure 6) and nucleosome structure (data not shown) seen a few hours after the shift is due to histone H3 hypoacetylation.

In the case of the triple mutant *rpd3*/*hda1*/*gcn5*, the delicate balance among the various acetyltransferases and deacetylases is such that in repressing conditions the structure of nucleosomes –1, +1 and +2 is loosened (Figure 3), correlating with the low amount of mRNA signal visible at 30 min and 1 h after the shift (see Figure 6).

Mechanisms of nucleosome modifications by changes in the histone acetylation level

How is the increased accessibility to MN of the two promoter nucleosomes achieved? One of the most common hypotheses deals with the decreased affinity for DNA of the nucleosome particle embedding hyperacetylated histones H3 and H4. In fact, hyperacetylated chromatin adopts a more 'open' structure (Garcia-Ramirez *et al*., 1995) and was shown to be generally sensitive to DNase I *in vivo* (Hebbes *et al*., 1994). In recent work, it was shown that hyperacetylated nucleosomes, isolated from HeLa cells grown in butyrate to inhibit all cellular deacetylases, affect the equilibrium constants for site exposure to restriction enzyme cleavage at various positions throughout the nucleosome (Anderson *et al*., 2001). The effect of histone acetylation on nucleosome–nucleosome interactions has not been defined, although internucleosomal contacts involving the N-terminal tails are likely to have a significant impact on higher order chromatin structure (Annunziato and Hansen, 2000).

Alternatively, the acetylation of specific lysine residues could serve as a marker for the binding of proteins required for a subsequent step in the transcription process (Strahl and Allis, 2000; Marmorstein, 2001). By using purified systems, it was shown that histone acetylation facilitates RNA polymerase II transcription in chromatin (Nightingale *et al*., 1998). *In vitro* evidence suggests that the H3/H4 tails are the primary arbiters of transcription factor access to intranucleosomal DNA (Vettese-Dadey *et al*., 1996; Howe *et al*., 1998; Vitolo *et al*., 2000). More recently, histone acetylation by either SAGA or NuA4 HAT complexes was shown to stabilize SWI/SNF binding

to promoter nucleosomes (Hassan *et al*., 2001). The specific timing for the targeting of these complexes *in vivo* was studied in detail in the case of a cell cycle-regulated *S.cerevisiae* promoter (Cosma *et al*., 1999; Krebs *et al*., 1999).

In the case of the *ADH2* promoter, we tested whether recruitment of TBP could be favored when the TATA box-containing nucleosome was remodeled in an *rpd3*- and *hda1*-dependent manner. However, we did not observe any increase in the occupancy of the promoter by TBP (Figure 5), suggesting that another factor, capable of inducing faster kinetics of activation in the *rpd3*, *hda1* and *rpd3*/*hda1* strains, is being recruited. This factor turned out to be the Adr1 protein itself, whose binding to the *ADH2* UAS1 is inhibited by glucose (Figure 4; Sloan *et al*., 1999), presumably by means of the TATA box-containing nucleosome. Nevertheless, only after the glucose content of the medium is lowered does the activator recruit the transcription machinery and the mRNA synthesis begin. In this way, the facilitated recruitment of Adr1 in repressing conditions determines faster kinetics of activation soon after the metabolic switch.

A model for the control of Adr1 chromosomal localization

The position of both UAS1 and UAS2 in the *ADH2* promoter is such that apparently there is no need to invoke a reorganization of the chromatin structure in order to allow the access of the activator to the promoter. They both are, in fact, located in a nucleosome-free region (Verdone *et al*., 1996). However, if one analyzes the exact location of the more upstream borders of the TATA box-containing –1 nucleosome (Verdone *et al*., 1996), it turns out that the left Adr1 consensus site in the UAS1 palindromic sequence is more accessible than the right one. Considering that the protein is quite large (1323 amino acids), one could expect some kind of steric hindrance exerted by the nucleosome particle on the binding of the second Adr1 molecule at the right consensus site. The present finding that Adr1 is not present on the wild-type promoter in high-glucose medium (Figure 4), but can bind in the same conditions in a strain carrying a disruption in both *HDA1* and *RPD3* histone deacetylases (Figure 5), points to the possibility that the repressive glucose effect is exerted, at least in part, at the DNA binding domain level by the presence of a defined nucleosome structure. When the TATA box-containing nucleosome is covalently modified by *GCN5*- and/or *ESA1*-mediated hyperacetylation, it becomes destabilized (as proposed; see Chiang *et al*., 1996), already allowing Adr1 to be correctly localized on the chromosome under repressing conditions. Nevertheless, TBP is not recruited in these conditions, suggesting that the access of the transcriptional activator to its target sites represents an essential but not sufficient regulatory step for *ADH2* derepression.

Histone deacetylation/acetylation is, therefore, directly involved in altering the chromatin structure at the *ADH2* promoter, influencing the binding of the major transcriptional activator with a concomitant effect on the kinetics of mRNA accumulation.

Materials and methods

Yeast strains and media

Saccharomyces cerevisiae strains used in this work are WJY139 (*MAT***a** *trp1-1 his3-11,15 ade2-1 leu2-1 can1-100 gcn5::URA3*), WJY140 (*MAT***a** *trp1-1 his3-11,15 ade2-1 ura3-52 can1-100 rpd3::LEU2*), WJY111 (*MAT***a** *ura3-52 his3-11,15 ade2-1 leu2-1 can1-100 hda1::TRP1*), WJY141 (*MAT***a** *ura3-52 his3-11,15 ade2-1 can1-100 rpd3::LEU2*, *hda1::TRP1*), WJY142 (*MAT***a** *his3-11,15 ade2-1 leu2-1 can1-100 hda1::TRP1*, *gcn5::URA3*), WJY143 (*MAT***a** *trp1-1 his3-11,15 ade2-1 can1-100 rpd3::LEU2*, *gcn5::URA3*) and WJY149 (*MAT***a** *his3-11,15 ade2-1 can1-100 rpd3::LEU2, hda1::TRP1*, *gcn5::URA3*). All these mutants are isogenic to YDS2 (Laman *et al*., 1995).

LPY3430 (*MAT***a** *his3Δ200 leu2-3,112 trp1Δ1 ura3-52 esa1::HIS3*, *esa1-L327S::URA3*) and LPY3431 (*MAT***a** *his3Δ200 leu2-3,112 trp1Δ1 ura3-52*, ESA1) were kindly provided by L.Pillus (Clarke *et al*., 1999). NSY164 (*rpd3*) and NSY165 (*rpd3*/*esa1*^{ts}) were constructed by deleting RPD3 in LPY3431 and LPY3430, respectively (Suka *et al*., 2001).

W303-1a (*MAT***a** *ade2 CAN1-100 his3-11,15 leu 2-13,112 trp1-1 ura3-1*), TYY202 (W303-1a *adr1::LEU2*) and KVRY9 (W303-1b *MAT*α ADR1-HAX3 *KAN*^{r} *ade2 CAN1-100 his3-11,15 leu2-13,112 trp1-1 ura3-1*) were used to test Adr1 and TBP occupancy of the *ADH2* promoter.

Yeast strains were grown in YPD medium (1% yeast extract, 2% bacto peptone, 3% glucose). To obtain *ADH2* derepression, the cells were collected by centrifugation, washed once with water, and resuspended in the same volume of fresh YP medium containing 0.05% glucose for the appropriate time.

Chromatin analysis

The analysis of nucleosome position and/or structure was performed using MN digestion of spheroplasts coupled with the indirect end-labeling procedure (Wu, 1980). Cells growing exponentially (A_{600} = 0.3 OD/ml) in *ADH2* repressing (3% glucose) or derepressing (0.05% glucose) conditions were washed once with water and then resuspended in zymolyase buffer (1 M sorbitol, 50 mM Tris–HCl pH 7.5, 10 mM β-mercaptoethanol). Incubation with zymolyase (0.01 mg/OD) was for 20 min at room temperature. The resulting spheroplasts were collected by centrifugation and resuspended in nystatin buffer (1 M sorbitol, 20 mM Tris–HCl pH 8.0, 1.5 mM $CaCl_2$, 50 mM NaCl, 100 μg/ml nystatin) in order to permeabilize cell membranes for the subsequent treatment with MN (Venditti and Camilloni, 1994). Incubation with MN was for 15 min at 37°C and the reaction was stopped with 5 mM EDTA, 1% SDS (final concentrations). The samples were then treated with proteinase K for 2 h at 56°C and purified by phenol–chloroform extraction and ethanol precipitation.

After secondary digestion with the appropriate restriction endonuclease, the samples were run on 1.5% agarose gels in TBE buffer and transferred to nitrocellulose filters. Southern blotting and hybridization were performed by standard procedures.

pFA plasmid DNA (Verdone *et al*., 1997) was used to prepare the probe for the indirect end-labeling analysis and as deproteinized material for control reactions with MN.

RNA analysis

Aliquots containing the same number of cells were collected by centrifugation, and total RNA was prepared as described previously (Schmitt *et al*., 1990). After spectrophotometric determination of the amount of RNA present in each aliquot, 10 μg of RNA were loaded onto 1.2% agarose–MOPS gels containing formaldehyde and ethidium bromide.

Northern blot analysis was performed by standard procedures. For hybridization, a 5′-end-labeled oligonucleotide (5′-GTTGGTAGCCT-TAACGACTGCGCTAAC-3′), specific for the *ADH2* gene (from +710 to +684 of the coding region), was used.

ChIP with anti-acetylated histone antibodies and PCR analyses

Highly specific antibodies raised against individual sites of acetylation were as described previously (Suka *et al*., 2001). ChIP and PCR reactions were carried out as described previously (Rundlett *et al*., 1998; Hecht and Grunstein, 1999) with some modifications (Suka *et al*., 2001). All the primers were designed as 24mers with ~50% GC content.

[α-^{32}P]dATP was added to the PCR reaction (1 μCi/12.5 μl) for quantification by PhosphorImager and ImageQuant software (Molecular Dynamics, Sunnyvale, CA).

ChIP with anti-Adr1 and anti-TBP antibodies and PCR analyses

ADR1 was tagged with a triple HA epitope using pUG6 (KAN) in strain W303-1b to create KVRY9 (the anti-HA_3Adr1 antibody was used for the experiment shown in Figure 4A). The anti-Adr1 antibody (used for the experiment shown in Figure 5C) is described in Dombek *et al*. (1993); the antibody against yeast TBP was kindly provided by S.Hahn. Chromatin was prepared as described previously (Kuras and Struhl, 1999; Li *et al*., 1999). Glycine was added to a final concentration of 330 mM. The concentration of NaCl was adjusted from 150 to 275 mM during incubation with the anti-TBP antibody. Immunoprecipitated DNA was analyzed by PCR using primer pairs for specific regions. Multiple PCR reactions were performed in order to check the linear range of amplification for each primer set and DNA sample. Reactions were carried out in 25 µl and contained 70 pmol of each primer, 200 µM dNTPs and 1 µCi of [α-^{32}P]dATP (sp. act. 3000 Ci/mmol). Cycling was for 5 min at 94°C, followed by 21 cycles with 30 s at 94°C, 30 s at 56°C, 1 min at 72°C, then 4 min at 72°C. PCR products were quantified using PhosphorImager and ImageQuant software (Molecular Dynamics).

Acknowledgements

We thank S.Venditti and G.Camilloni for helpful discussions, and C.Presutti for critical reading of the manuscript. This work was supported by grants from CNR TP on Biotechnology, MURST 40% 2001, MURST 5% 'BSU', NIH GM 26079 to E.T.Y. and NIH GM 23674 to M.G.

References

Aalfs,J.D. and Kingston,R.E. (2000) What does 'chromatin remodeling' mean? *Trends Biochem. Sci.*, **25**, 548–555.

Allard,S., Utley,R.T., Savard,J., Clarke,A., Grant,P., Brandl,C.J., Pillus,L., Workman,J.L. and Côté,J. (1999) NuA4, an essential transcription adaptor/histone H4 acetyltransferase complex containing Esa1p and the ATM-related cofactor Tra1p. *EMBO J.*, **18**, 5108–5119.

Anderson,J.D., Lowary,P.T. and Widom,J. (2001) Effects of histone acetylation on the equilibrium accessibility of nucleosomal DNA target sites. *J. Mol. Biol.*, **307**, 977–985.

Annunziato,A.T. and Hansen,J.C. (2000) Role of histone acetylation in the assembly and modulation of chromatin structures. *Gene Expr.*, **9**, 37–61.

Beier,D.R. and Young,E.T. (1982) Characterization of a regulatory region upstream of the *ADR2* locus of *S. cerevisiae*. *Nature*, **300**, 724–728.

Braunstein,M., Rose,A.B., Holmes,S.G., Allis,C.D. and Broach,J.R. (1993) Transcriptional silencing in yeast is associated with reduced nucleosome acetylation. *Genes Dev.*, **7**, 592–604.

Chiang,Y.-C., Komarnitsky,P., Chase,D. and Denis,C.L. (1996) ADR1 activation domains contact the histone acetyltransferase GCN5 and the core transcriptional factor TFIIB. *J. Biol. Chem.*, **271**, 32359–32365.

Clarke,A.S., Lowell,J.E., Jacobson,S.J. and Pillus,L. (1999) Esa1p is an essential histone acetyltransferase required for cell cycle progression. *Mol. Cell. Biol.*, **19**, 2515–2526.

Cosma,M.P., Tanaka,T. and Nasmyth,K. (1999) Ordered recruitment of transcription and chromatin remodeling factors to a cell cycle- and developmentally regulated promoter. *Cell*, **97**, 299–311.

Deckert,J. and Struhl,K. (2001) Histone acetylation at promoters is differentially affected by specific activators and repressors. *Mol. Cell. Biol.*, **21**, 2726–2735.

Denis,C.L. and Young,E.T. (1983) Isolation and characterization of the positive regulatory gene *ADR1* from *Saccharomyces cerevisiae*. *Mol. Cell. Biol.*, **3**, 360–370.

DiMauro,E., Kendrew,S.G. and Caserta,M. (2000) Two distinct nucleosome alterations characterize chromatin remodeling at the *Saccharomyces cerevisiae ADH2* promoter. *J. Biol. Chem.*, **275**, 7612–7618.

Dombek,K.M., Camier,S. and Young,E.T. (1993) *ADH2* expression is repressed by REG1 independently of mutations that alter the phosphorylation of the yeast transcription factor ADR1. *Mol. Cell. Biol.*, **13**, 4391–4399.

Garcia-Ramirez,M., Rocchini,C. and Ausio,J. (1995) Modulation of chromatin folding by histone acetylation. *J. Biol. Chem.*, **270**, 17923–17928.

Grant,P.A. *et al*. (1997) Yeast Gcn5 functions in two multisubunit complexes to acetylate nucleosomal histones: characterization of an Ada complex and the SAGA (Spt/Ada) complex. *Genes Dev.*, **11**, 1640–1650.

Hamiche,A., Sandaltzopoulos,R., Gdula,D.A. and Wu,C. (1999) ATP-dependent histone octamer sliding mediated by the chromatin remodeling complex NURF. *Cell*, **97**, 833–842.

Hassan,H., Neely,K.E. and Workman,J.L. (2001) Histone acetyltransferase complexes stabilize SWI/SNF binding to promoter nucleosomes. *Cell*, **104**, 817–827.

Hebbes,T.R., Clayton,A.L., Thorne,A.W. and Crane-Robinson,C. (1994) Core histone acetylation co-maps with generalized DNase I sensitivity in the chicken β-globin chromosomal domain. *EMBO J.*, **13**, 1823–1830.

Hecht,A. and Grunstein,M. (1999) Mapping DNA interaction sites of chromosomal proteins using immunoprecipitation and polymerase chain reaction. *Methods Enzymol.*, **304**, 399–414.

Hirschhorn,J.N., Brown,S.A., Clark,C.D. and Winston,F. (1992) Evidence that *SNF2/SWI2* and *SNF5* activate transcription in yeast by altering chromatin structure. *Genes Dev.*, **6**, 2288–2298.

Howe,L., Ranalli,T.A., Allis,C.D. and Ausio,J. (1998) Transcriptionally active *Xenopus laevis* somatic 5 S ribosomal RNA genes are packaged with hyperacetylated histone H4, whereas transcriptionally silent oocyte genes are not. *J. Biol. Chem.*, **273**, 20693–20696.

Kadosh,D. and Struhl,K. (1998) Histone deacetylase activity of *RPD3* is important for transcriptional repression *in vivo*. *Genes Dev.*, **12**, 797–805.

Kingston,R.E. and Narlikar,G.J. (1999) ATP-dependent remodeling and acetylation as regulators of chromatin fluidity. *Genes Dev.*, **13**, 2339–2352.

Kornberg,R.D. and Lorch,Y. (1999) Chromatin-modifying and -remodeling complexes. *Curr. Opin. Genet. Dev.*, **9**, 148–151.

Krebs,J.E., Kuo,M.-H., Allis,C.D. and Peterson,C.L. (1999) Cell cycle-regulated histone acetylation required for expression of the yeast HO gene. *Genes Dev.*, **13**, 1412–1421.

Kuo,M., Zhou,J., Jambeck,P., Churchill,M.E.A. and Allis,C.D. (1998) Histone acetyltransferase activity of Gcn5p is required for the activation of target genes *in vivo*. *Genes Dev.*, **12**, 627–639.

Kuo,M.-H., vom Baur,E., Struhl,K. and Allis,C.D. (2000) Gcn4 activator targets Gcn5 histone acetyltransferase to specific promoters independently of transcription. *Mol. Cell*, **6**, 1309–1320.

Kuras,L. and Struhl,K. (1999) Binding of TBP to promoters *in vivo* is stimulated by activators and requires Pol II holoenzyme. *Nature*, **399**, 609–613.

Laman,H., Balderes,D. and Shore,D. (1995) Disturbance of normal cell cycle progression enhances the establishment of transcriptional silencing in *Saccharomyces cerevisiae*. *Mol. Cell. Biol.*, **15**, 3608–3617.

Längst,G., Bonte,E.J., Corona,D.F.V. and Becker,P.B. (1999) Nucleosome movement by CHRAC and ISWI without disruption or *trans*-displacement of the histone octamer. *Cell*, **97**, 843–852.

Li,X.-Y., Virbasius,A., Zhu,X. and Green,M. (1999) Enhancement of TBP binding by activators and general transcription factors. *Nature*, **399**, 605–609.

Litt,M.D., Simpson,M., Recillas-Targa,F., Prioleau,M.-N. and Felsenfeld,G. (2001) Transitions in histone acetylation reveal boundaries of three separately regulated neighboring loci. *EMBO J.*, **20**, 2224–2235.

Lorch,Y., Zhang,M. and Kornberg,R.D. (1999) Histone octamer transfer by a chromatin-remodeling complex. *Cell*, **96**, 389–392.

Marmorstein,R. (2001) Protein modules that manipulate histone tails for chromatin regulation. *Nature Rev. Mol. Cell. Biol.*, **2**, 422–432.

Nightingale,K.P., Wellinger,R.E., Sogo,J.M. and Becker,P.B. (1998) Histone acetylation facilitates RNA polymerase II transcription of the *Drosophila hsp26* gene in chromatin. *EMBO J.*, **17**, 2865–2876.

Peterson,C.L. and Herskowitz,I. (1992) Characterization of the yeast *SWI1*, *SWI2* and *SWI3* genes, which encode a global activator of transcription. *Cell*, **68**, 573–583.

Reinke,H., Gregory,P.D. and Hörz,W. (2001) A transient histone hyperacetylation signal marks nucleosomes for remodeling at the *PHO8* promoter *in vivo*. *Mol. Cell*, **7**, 529–536.

Rundlett,S.E., Carmen,A.A., Kobayashi,R., Bavykin,S., Turner,B. and Grunstein,M. (1996) *HDA1* and *RPD3* are members of distinct yeast histone deacetylase complexes that regulate silencing and transcription. *Proc. Natl Acad. Sci. USA*, **93**, 14503–14508.

Rundlett,S.E., Carmen,A.A., Suka,N., Turner,B.M. and Grunstein,M. (1998) Transcriptional repression by *UME6* involves deacetylation of lysine 5 of histone H4 by *RPD3*. *Nature*, **392**, 831–835.

Schmitt,M.E., Brown,T.A. and Trumpower,B.L. (1990) A rapid and simple method for preparation of RNA from *Saccharomyces cerevisiae*. *Nucleic Acids Res.*, **18**, 3091.

Sloan,J.S., Dombeck,K.M. and Young,E.T (1999) Post-translational regulation of Adr1 activity is mediated by its DNA binding domain. *J. Biol. Chem.*, **274**, 37575–37582.

Smith,E.R., Eisen,A., Gu,W., Sattah,M., Pannuti,A., Zhou,J., Cook,R.G., Lucchesi,J.C. and Allis,C.D. (1998) *ESA1* is a histone acetyltransferase that is essential for growth in yeast. *Proc. Natl Acad. Sci. USA*, **95**, 3561–3565.

Strahl,B.D. and Allis,C.D. (2000) The language of covalent histone modifications. *Nature*, **403**, 41–45.

Struhl,K. (1998) Histone acetylation and transcriptional regulatory mechanisms. *Genes Dev.*, **12**, 599–606.

Suka,N., Suka,Y., Carmen,A.A., Wu,J. and Grunstein,M. (2001) Highly specific antibodies determine histone acetylation site usage in yeast heterochromatin and euchromatin. *Mol. Cell*, **8**, 473–479.

Travers,A.A. (1999) An engine for nucleosome remodeling. *Cell*, **96**, 311–314.

Venditti,S. and Camilloni,G. (1994) *In vivo* analysis of chromatin following nystatin-mediated import of active enzymes into *Saccharomyces cerevisiae*. *Biochim. Biophys. Acta*, **1219**, 677–689.

Verdone,L., Camilloni,G., Di Mauro,E. and Caserta,M. (1996) Chromatin remodeling during *Saccharomyces cerevisiae ADH2* gene activation. *Mol. Cell. Biol.*, **16**, 1978–1988.

Verdone,L., Cesari,F., Denis,C.L., Di Mauro,E. and Caserta,M. (1997) Factors affecting *Saccharomyces cerevisiae ADH2* chromatin remodeling and transcription. *J. Biol. Chem.*, **272**, 30828–30834.

Vettese-Dadey,M., Grant,P.A., Hebbes,T.R., Craine-Robinson,C., Allis,C.D. and Workman,J.L. (1996) Acetylation of histone H4 plays a primary role in enhancing transcription factor binding to nucleosomal DNA *in vitro*. *EMBO J.*, **15**, 2508–2518.

Vignali,M., Hassan,A.H. and Workman,J.L (2000) ATP-dependent chromatin-remodeling complexes. *Mol. Cell. Biol.*, **20**, 1899–1910.

Vitolo,J.M., Thiriet,C. and Hayes,J.J. (2000) The H3–H4 N-terminal tail domains are the primary mediators of transcription factor IIIA access to 5 S DNA within a nucleosome. *Mol. Cell. Biol.*, **20**, 2167–2175.

Vogelauer,M., Wu,J., Suka,N. and Grunstein,M. (2000) Global histone acetylation and deacetylation in yeast. *Nature*, **408**, 495–498.

Whitehouse,I., Flaus,A., Cairns,B.R., White,M.F., Workman,J.L. and Owen-Hughes,T. (1999) Nucleosome mobilization catalyzed by the yeast SWI/SNF complex. *Nature*, **400**, 784–787.

Wu,C. (1980) The 5′ ends of *Drosophila* heat shock genes in chromatin are hypersensitive to DNase I. *Nature*, **286**, 854–860.

Wu,J. and Grunstein,M. (2000) 25 years after the nucleosome model: chromatin modifications. *Trends Biochem. Sci.*, **25**, 619–623.

Wu,J., Suka,N., Carlson,M. and Grunstein,M. (2001) TUP1 utilizes histone H3/H2B-specific HDA1 deacetylase to repress gene activity in yeast. *Mol. Cell*, **7**, 117–126.

Wyrick,J.J., Holstege,F.C., Jennings,E.G., Causton,H.C., Shore,D., Grunstein,M., Lander,E.S. and Young,R.A. (1999) Chromosomal landscape of nucleosome-dependent gene expression and silencing in yeast. *Nature*, **402**, 418–421.

Received November 15, 2001; revised and accepted January 11, 2002